NASA TM X-654

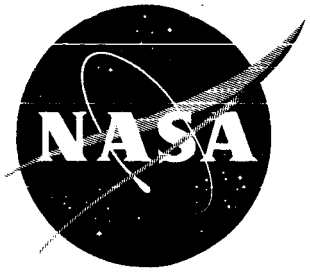

TECHNICAL MEMORANDUM

X-654

WIND-TUNNEL MEASUREMENTS AT MACH NUMBERS FROM 3 TO 5 OF PRESSURE AND TURBULENT HEAT TRANSFER ON A BLUNT CONE-CYLINDER WITH FLARED AFTERBODY

By Mamoru Inouye and John B. Sisk

Ames Research Center
Moffett Field, Calif.

CLASSIFIED DOCUMENT - TITLE UNCLASSIFIED

This material contains information affecting the national defense of the United States within the meaning of the espionage laws, Title 18, U.S.C., Secs. 793 and 794, the transmission or revelation of which in any manner to an unauthorized person is prohibited by law.

NATIONAL AERONAUTICS AND SPACE ADMINISTRATION

WASHINGTON July 1962

NATIONAL AERONAUTICS AND SPACE ADMINISTRATION

TECHNICAL MEMORANDUM X-654

WIND-TUNNEL MEASUREMENTS AT MACH NUMBERS FROM 3 TO 5 OF PRESSURE AND TURBULENT HEAT TRANSFER ON A BLUNT CONE-CYLINDER WITH FLARED AFTERBODY*

By Mamoru Inouye and John B. Sisk

SUMMARY

Wind-tunnel tests were conducted at Mach numbers of 3.03, 4.10, and 5.00 on a blunt cone-cylinder model with a flared afterbody. The data were compared with numerical flow-field calculations which consisted of a blunt-body solution joined with the method of characteristics. The bow-wave configurations and surface pressure distributions were predicted well for all Mach numbers except where viscous effects were present. Turbulent heat-transfer measurements on the cone and cylinder at a Mach number of 3.03 and a free-stream Reynolds number based on cylinder diameter of 1.08×10^6 agreed well with the predictions of Vaglio-Laurin and the reference temperature method; the heat-transfer rates measured on the flare were somewhat higher than the predicted values.

Predictions of surface pressures agreed well with previously reported flight data for the same configuration at a Mach number of 10. Turbulent heat-transfer rates to the flight model were predicted well with the Vaglio-Laurin theory.

INTRODUCTION

Knowledge of turbulent boundary-layer heating rates is important for the design of hypersonic vehicles, and the major portion of such knowledge has been supplied by experimental investigations. Although wind-tunnel tests seldom duplicate simultaneously the flight conditions of Mach number, Reynolds number, and total enthalpy, they provide not only the heat-transfer rates but also the flow conditions at the outer edge of the boundary layer, both of which are necessary for assessing our understanding of the flow phenomena.

*Title, Unclassified

The present investigation was undertaken in conjunction with a flight test to study the heat transfer to the same representative blunt-nosed body. It was hoped that the combination of a limited amount of flight data and more detailed wind-tunnel data would provide sufficient information to indicate the appropriate method for predicting turbulent heat-transfer rates to blunt-nosed bodies. The results of the flight test, reported in reference 1, showed that the Vaglio-Laurin theory (ref. 2) predicted the heat-transfer rates well.

The purpose of this report is to present the pressure and turbulent heat-transfer data obtained in the Ames 10-Inch Heat Transfer Wind Tunnel and to compare them with the available theories.

SYMBOLS

c	specific heat, Btu/lb ^{o}R
d	cylinder diameter, ft
k	thermal conductivity, Btu/(sec ft^2 ^{o}R/ft)
M	Mach number
Nu	Nusselt number, $\frac{q_w s}{k_s(T_r - T_w)}$
p	static pressure, lb/ft^2
p_t	total pressure, lb/ft^2
q	heat-transfer rate per unit area, Btu/sec ft^2
Re_∞	Reynolds number based on free-stream conditions and cylinder diameter, $\frac{\rho_\infty V_\infty d}{\mu_\infty}$
Re_s	Reynolds number based on stagnation point conditions and distance along surface, $\frac{s}{\mu_s}\sqrt{\rho_s p_s}$
s	distance along surface measured from stagnation point, ft
T	temperature, ^{o}R
T_r	recovery temperature, ^{o}R
V	velocity, ft/sec
x, r	cylindrical coordinates with origin at stagnation point, ft

γ ratio of specific heats

ρ density, lb sec^2/ft^4

τ wall thickness, in.

μ viscosity, lb sec/ft^2

Subscripts

s stagnation point on model

w wall

∞ free stream

MODELS

The blunt-nosed shape tested is shown in figure 1. It is a one-third scale model of the flight test model of reference 1. Two models were constructed, one to measure surface pressures and the other to measure heat-transfer rates.

The pressure model was machined from mild steel with a wall thickness of approximately 1/4 inch. Twenty-one pressure taps were located on a meridian with three additional taps equally spaced circumferentially at a cone station as tabulated in figure 1. Stainless steel tubing, 0.030 inch I.D., was used for the pressure leads. The tubing was soldered in holes drilled in the model surface and finished to leave a 0.030-inch diameter orifice.

The heat-transfer model was a thin-walled shell, approximately 0.030 inch thick, machined from 17-4 PH stainless steel. Twenty-four chromel-constantan thermocouples were installed at locations near those corresponding to the pressure taps. The location and the wall thickness of each station are tabulated in figure 1. Each thermocouple junction was formed by soldering the two 0.005-inch diameter leads in holes drilled 1/8 inch apart circumferentially.

A trip was employed on both models to obtain a turbulent boundary layer. The trip was a circular piece of 1/0 garnet paper with nearly all the backing sanded off and glued to the subsonic portion of the spherical nose. Except for the stagnation point pressure tap which was drilled out, the first two thermocouple and pressure stations were covered by the trip.

[redacted]

TEST PROCEDURE

The tests were conducted in the Ames 10-Inch Heat Transfer Wind Tunnel which is of the continuous flow type with variable Mach number (3 to 5) and stagnation pressure. A sketch and description of the facility can be found in reference 3. The models were tested at zero angle of attack at Mach numbers of 3.03, 4.10, and 5.00, a nominal stagnation temperature of 660° R, and free-stream Reynolds numbers based on cylinder diameter from 0.54×10^6 to 1.08×10^6.

Tests with the pressure model included measurements of surface pressures and impact pressures in the boundary layer. The latter were obtained at stations 14, 16, 18, and 20 to 24 with the probe assembly and pressure recording apparatus described in reference 4. Two different probe tips were used with over-all heights of 0.006 and 0.008 inch.

A transient technique was used to obtain the heat-transfer results. Liquid nitrogen was introduced in the tunnel air stream to initially cool the model approximately 50° F below the equilibrium temperature. Then the nitrogen flow was stopped, and the model was allowed to heat to equilibrium temperature. During this heating period, the model temperatures and their time derivatives were recorded on an oscillograph.

The following procedure was used to calculate the heat-transfer coefficients. If the radiation to the tunnel walls and radial conduction through the model wall are assumed to be negligible, an energy balance per unit surface area at a thermocouple station yields

$$q_w = q_{stored} - q_{cond}$$

where q_w is the convection heat-transfer rate, q_{stored} is the rate of change of heat stored in the mass considered, and q_{cond} is the conduction loss rate. The q_{stored} term was calculated from the time derivative of the temperature, wall thickness, and specific heat of the wall material. Since the specific heat varies with temperature, it was obtained from tests conducted by Battelle Memorial Institute on a sample piece of 17-4 PH stainless steel. The results are shown in figure 2. With the circumferential conduction estimated to be negligible, the conduction corrections were limited to the axial direction. To calculate the q_{cond} term for a given station a fourth-degree polynomial was then fitted to the temperatures recorded at four adjacent stations. For the test conditions of $M_\infty = 3.03$ and $Re_\infty = 1.08\times10^6$, q_{cond} was on the average one-fifth of q_w. The resulting q_w was plotted versus the temperature for each station. When the heat-transfer coefficient was constant, the plot was a straight line with the slope representing the heat-transfer coefficient and the intercept for zero heat transfer representing the recovery temperature.

[redacted]

RESULTS AND DISCUSSION

Shock-Wave Shape

The shock-wave configurations around the model for $M_\infty = 3.03$, 4.10, and 5.00 are shown in figure 3. The experimental points were obtained from schlieren pictures and impact pressure surveys of the flare shock wave. The radial coordinates of the measured shock shapes agree within 5 percent with the results of a numerical calculation of the inviscid flow field which consisted of a blunt-body solution found according to reference 5 and a continuation of the solution in the supersonic region using the method of characteristics. The measured bow shock always lies outside the calculated shock shape, indicating that the discrepancy could be attributed partly to the boundary-layer displacement effect which was ignored in the calculations. However, the spread in the data because of difficulties in reading and interpreting different schlieren pictures is of the same magnitude. The flow around the flare was treated approximately; the flow field ahead of the flare shock wave was assumed to be uniform. In these calculations the Mach number on the surface at the aft portion of the cylinder was used for the uniform flow field. In reality, the Mach number increases away from the surface and should cause the shock wave to lie closer to the aft portion of the flare than calculated and hence to be in closer agreement with the measurements for $M_\infty = 3.03$ and 4.10. For $M_\infty = 5.00$ separation of the boundary layer disrupted the flare shock wave, and no measurements were made. Although the calculated radial coordinates of the flare shock wave agree fairly well with the measured values, the slopes, which really determine the flow behind the shock wave, are quite different.

Surface Pressure

The static-pressure distributions for $M_\infty = 3.03$, 4.10, and 5.00 are shown in figure 4. In general, good agreement exists between the experimental results and the previously described numerical calculations. On the sphere the boundary-layer trip probably disturbed the flow locally and caused the poor agreement between the experimental and theoretical results. On the cone the agreement is very good. On the cylinder where the viscous effects were more pronounced, the calculation method underestimates the pressure as expected, but the agreement is still good. At the higher Mach numbers the boundary layer was not fully turbulent, despite the nose trip, and separation occurred ahead of the flare. This fact was substantiated by some impact pressure surveys not shown in this report.

On the flare the calculation method predicts the magnitude of the surface pressures, but not the gradient. As noted in the discussion of the shock-wave shape, the calculations for the flare are not exact because it was necessary to assume a uniform flow field ahead of the flare shock wave equal to that existing on the aft portion of the cylinder. Consequently, the calculations underestimate the pressure on the rear part of the flare because in fact the Mach number and total pressure of the flow field actually increase away from the surface of the cylinder. For $M_\infty = 5.00$, appreciable separation of the boundary layer occurred, and the results cannot be compared with the numerical calculations.

In view of the good agreement between the wind-tunnel data and the numerical calculations for the cone and cylinder, the question arises as to whether or not the method can be applied to flight data. In figure 5 the flight data from reference 1 for the same model configuration are compared with the numerical calculations for $M_\infty = 10$ and $\gamma = 1.4$. For the flight conditions the air at the stagnation point was dissociated approximately 2 percent with an effective γ of 1.2. The spread in the flight data is the result of angles of attack of $\pm 1^\circ$. The Space Technology Laboratories' calculations for the pressure distribution, as described in reference 1, are also shown in figure 5. The equilibrium properties of air were used in these calculations but with an approximate technique to start the method of characteristics rather than an exact solution as reported erroneously in reference 1. The flow around the flare was treated properly since the nonuniform flow field ahead of the flare shock wave was considered. In the present numerical calculations, an exact solution for the nose region was used, but the calculations required the assumption of a perfect gas with a constant ratio of specific heats. In addition, the flow field around the flare was found approximately. Both calculation methods predict the flight data within reasonable limits. It is noted that for a blunt-nosed slender body, such as considered here, the surface pressure distribution for flight conditions is substantially different from that existing for somewhat lower Mach number wind-tunnel conditions.

A 5 9 0

Total Pressure at Outer Edge of Boundary Layer

Other quantities besides the static pressure must be measured in order to determine the flow conditions at the outer edge of the boundary layer. The most convenient one is the impact pressure. The pitot tube equation can be used to calculate the local total pressure. Difficulty arises in determining the precise location of the edge of the boundary layer. Since the impact pressure in the inviscid flow was found to vary nearly linearly with distance from the surface, the boundary-layer edge was determined as the point where the impact pressure dropped from this line. In figure 6 the total pressure at the outer edge of the boundary layer determined from impact pressure surveys for $M_\infty = 3.03$ is compared

with the values given by the numerical calculations. The total pressure at the body surface ahead of the flare must theoretically be equal to the value at the stagnation point behind the normal shock wave because the body surface is a streamline, and the flow is assumed isentropic on a streamline. On the flare the total pressure is about 10 percent lower, the flow having passed through an oblique shock.

The total pressures measured at the outer edge of the boundary layer on the cylinder were approximately 10 percent higher than the theoretical values on the body surface. On the flare the measured total pressures were 25 to 50 percent higher than the theoretical values, even exceeding the value on the cylinder. A possible explanation for this rise in total pressure is that a streamline at the outer edge of the boundary layer does not pass through the normal shock wave at the nose but rather through an oblique shock wave with less loss of total pressure. Comparison of the total mass flow rate in the boundary layer with the free-stream flow rate through the known bow-wave shape showed that the rise in total pressure could be accounted for in this manner.

Heat Transfer

For $M_\infty = 4.10$ and 5.00, the boundary layer was transitional or separated. The heat-transfer rates on the cylinder did not vary linearly with surface temperature because of nonuniform surface temperature effects or because the character of the boundary layer was changing with temperature level. Hence, no heat-transfer coefficients could be calculated. Some results were obtained for the flare, but these are not presented because of the questionable nature of the flow.

The heat-transfer distributions for $M_\infty = 3.03$ are shown in figure 7 for Reynolds numbers based on free-stream conditions and cylinder diameters of 0.545×10^6, 0.799×10^6, and 1.08×10^6. The data for the first two stations are omitted because the thermocouples were covered by the boundary-layer trip. The results are compared with two predictions for turbulent flow, the Vaglio-Laurin theory (ref. 2) and the reference temperature method (ref. 6) with constants appropriate for turbulent flow obtained from reference 7. Also shown is a prediction for laminar flow by the method of Stine and Wanlass (ref. 8). With the exception of the laminar prediction for $Re_\infty = 0.54\times10^6$, the theoretical values were calculated for $M_\infty = 3.03$ and $Re_\infty = 1.08\times10^6$. A 50-percent decrease in the Reynolds number had negligible effect on the turbulent predictions. The flow conditions at the outer edge of the boundary layer necessary for the theoretical heat-transfer predictions were obtained from the experimental surface pressure distribution and impact pressure surveys where the latter were available. For the sphere and cone it was assumed that the total pressure at the outer edge of the boundary layer was equal to the stagnation-point pressure.

For the two lower Reynolds numbers the heat-transfer results on the cone and cylinder indicate laminar or transitional flow. For the highest Reynolds number, the results indicate turbulent flow after the center of the cone. Subsequent discussion of the results will be confined to this case.

For the cone, the Vaglio-Laurin theory and the reference temperature method predict the same heat-transfer rates and agree with the data within ±5 percent. For the cylinder, the reference temperature predictions are 10 percent higher than Vaglio-Laurin's. Both predictions show the same general agreement with the data. (Thermocouple no. 12 failed during the test.) For the flare, the Vaglio-Laurin theory predicts heat-transfer rates 10 percent higher than the reference temperature method but still lower than the data.

A 5 9 0

At least for the conical and cylindrical portions of the model, the Vaglio-Laurin theory and the reference temperature method predict well the turbulent heat transfer for wind-tunnel conditions. In reference 1 it was found that the Vaglio-Laurin theory also predicted well the heat transfer under flight conditions with $M_\infty = 10$. In figure 8 the flight test heat-transfer results are reproduced and compared again with theoretical predictions. The theoretical predictions shown in figure 8 differ from those in reference 1, in that the present calculation method was used to obtain the pressure distribution from which local flow conditions were determined. As expected, the Vaglio-Laurin theory predicts well the heat transfer to all parts of the model under flight conditions with the flow around the model calculated for a perfect gas. It is observed that similarly to the surface pressure distribution, the general level and distribution of turbulent heat-transfer rates (expressed nondimensionally as suggested by Vaglio-Laurin) differ for flight and wind-tunnel conditions.

SUMMARY OF RESULTS

Wind-tunnel tests were conducted at Mach numbers of 3.03, 4.10, and 5.00 on a blunt cone-cylinder model with a flared afterbody. The data were compared with numerical calculations of the inviscid flow field consisting of a blunt-body flow-field solution joined with the method of characteristics. The following results were obtained:

1. The radial coordinates of the bow-wave configurations were predicted within 5 percent for all Mach numbers.

2. The surface pressure distributions were predicted reasonably well for all Mach numbers except for the separated flow region ahead of the flare at a Mach number of 5.0.

3. At a Mach number of 3.03 the total pressure measured at the outer edge of the boundary layer on the cylinder was 10 percent higher than the theoretical value for the surface. The total pressure measured at the outer edge of the boundary layer on the flare was 25 to 50 percent higher than the theoretical value.

4. Turbulent heat-transfer data were obtained for a Mach number of 3.03 and a free-stream Reynolds number based on the cylinder diameter of 1.08×10^6. Comparison of the data with predictions by the theory of Vaglio-Laurin and by the reference temperature method showed good agreement for the conical and cylindrical portions. For the flare the Vaglio-Laurin theory showed the best agreement with the data.

5. The theoretical methods for predicting the pressure and turbulent heat transfer were also applied to the previously reported results of a flight test at a Mach number of 10 with the same configuration. Comparisons of the results again showed good agreement.

Ames Research Center
National Aeronautics and Space Administration
Moffett Field, Calif., April 10, 1962

[redacted]

REFERENCES

1. Inouye, Mamoru, and Neel, Carr B.: Free-Flight Measurements up to a Mach Number of 11 of Pressure and Turbulent Heat Transfer on a Blunted Cone-Cylinder With Flared Afterbody. NASA TM X-505, 1961.

2. Vaglio-Laurin, Roberto: Turbulent Heat Transfer on Blunt-Nosed Bodies in Two-Dimensional and General Three-Dimensional Hypersonic Flow. Jour. Aero/Space Sci., vol. 27, no. 1, Jan. 1960, pp. 27-36.

3. Tendeland, Thorval: Effects of Mach Number and Wall-Temperature Ratio on Turbulent Heat Transfer at Mach Numbers From 3 to 5. NACA TN 4236, 1958.

4. Tendeland, Thorval, Nielsen, Helmer L., and Fohrman, Melvin J.: The Flow Field Over Blunted Flat Plates and Its Effect on Turbulent Boundary-Layer Growth and Heat Transfer at a Mach Number of 4.7. NASA TN D-689, 1961.

5. Fuller, Franklyn B.: Numerical Solutions for Supersonic Flow of an Ideal Gas Around Blunt Two-Dimensional Bodies. NASA TN D-791, 1961.

6. Rubesin, Morris W., and Johnson, H. A.: A Critical Review of Skin-Friction and Heat-Transfer Solutions of the Laminar Boundary Layer of a Flat Plate. ASME Trans., vol. 71, no. 4, May 1949, pp. 383-8.

7. Sommer, Simon C., and Short, Barbara J.: Free-Flight Measurements of Turbulent-Boundary-Layer Skin Friction in the Presence of Severe Aerodynamic Heating at Mach Numbers From 2.8 to 7.0. NACA TN 3391, 1955.

8. Stine, Howard A., and Wanlass, Kent: Theoretical and Experimental Investigation of Aerodynamic-Heating and Isothermal Heat-Transfer Parameters on a Hemispherical Nose With Laminar Boundary Layer at Supersonic Mach Numbers. NACA TN 3344, 1954.

A 5 9 0

[redacted]

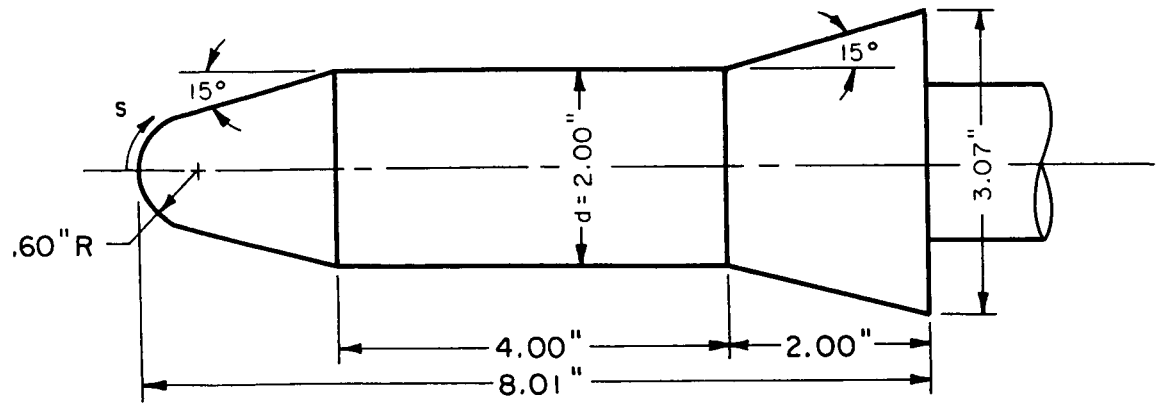

Station no.	Thermocouple		Pressure
	s/d	τ, in.	s/d
1	.031	.0315	0
2	.131	.0315	.125
3	.262	.0335	.235
s/d = 0.393, sphere - cone junction			
4	.455	.0260	.425
5	.605	.0260	.575
6	.780	.0260	.750
7	.955	.0265	.925
8	.955	.0265	.925
9	.955	.0265	.925
10	.955	.0265	.925
11	1.130	.0265	1.105
s/d = 1.206, cone - cylinder junction			
12	1.280	.0285	1.250
13	1.430	.0285	1.400
14	1.705	.0295	1.650
15	1.980	.0295	1.950
16	2.255	.0295	2.225
17	2.530	.0300	2.500
18	2.805	.0300	2.775
19	3.080	.0305	3.050
s/d = 3.206, cylinder - flare junction			
20	3.305	.0305	3.305
21	3.480	.0305	3.480
22	3.705	.0310	3.705
23	3.930	.0315	3.935
24	4.155	.0340	4.100
s/d = 4.240, base			

Figure 1.- Model configuration and instrumentation.

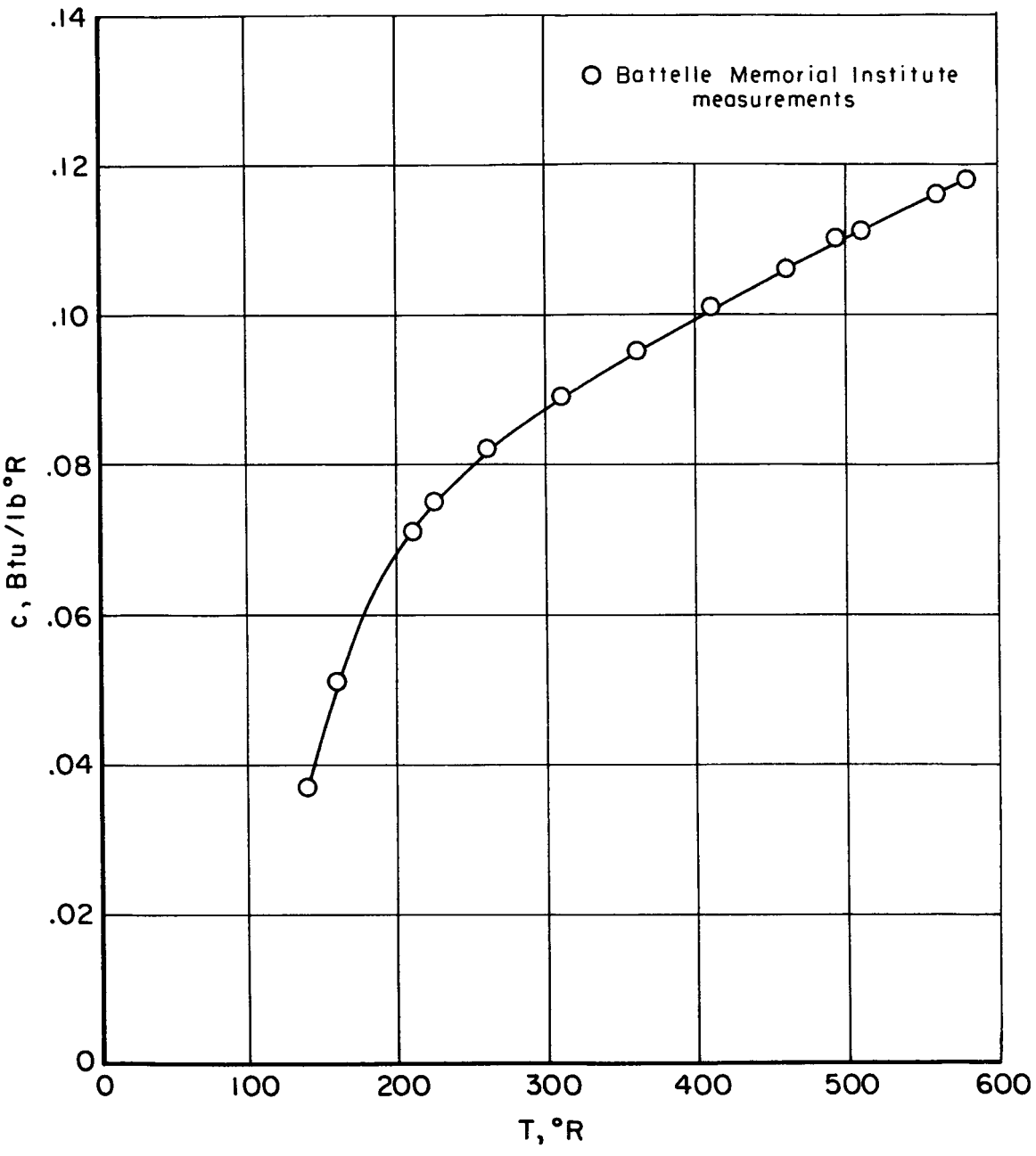

Figure 2.- Specific heat of 17-4 PH stainless steel as a function of temperature.

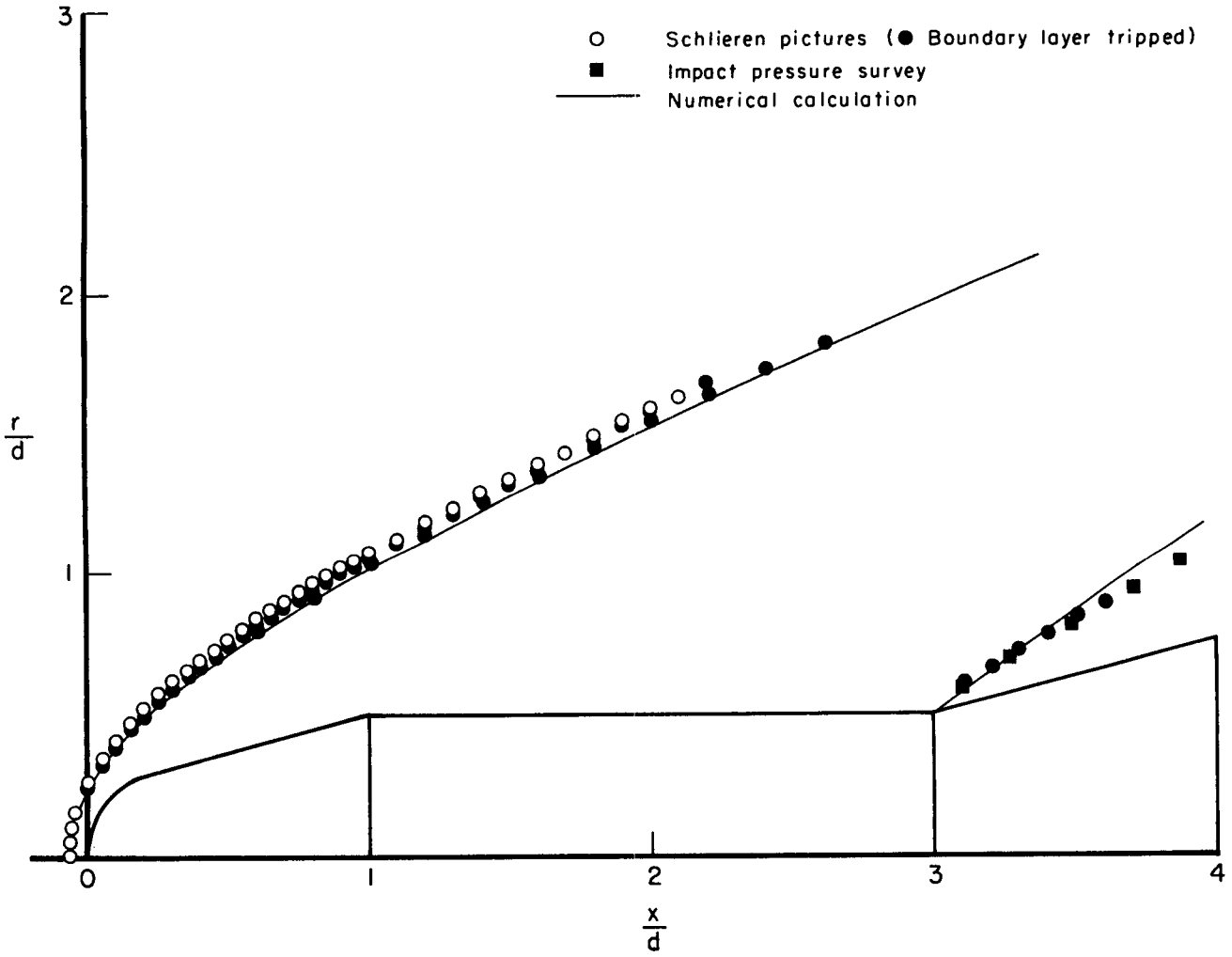

(a) $M_\infty = 3.03$, $\gamma = 1.4$

Figure 3.- Shock-wave shape.

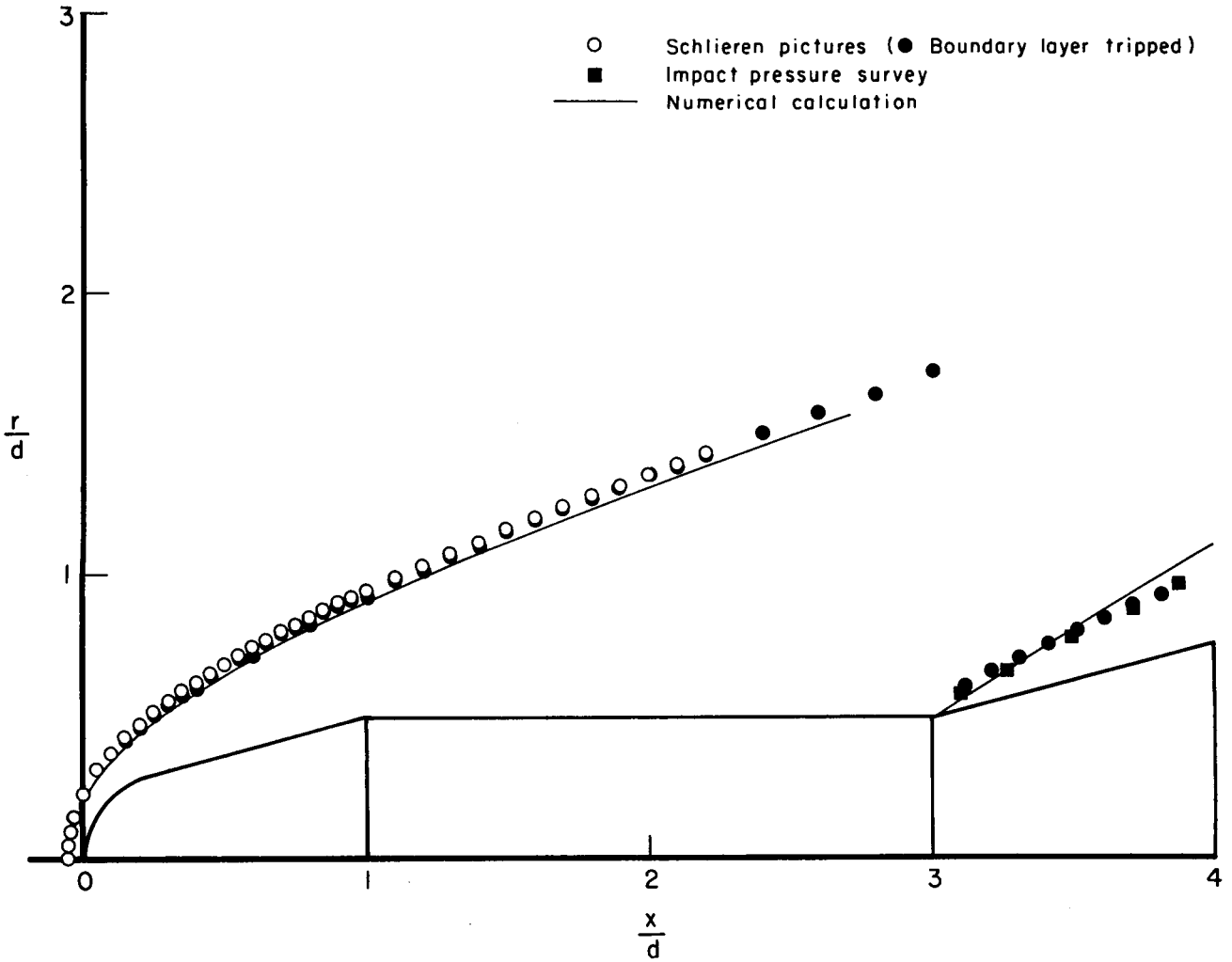

(b) $M_\infty = 4.10$, $\gamma = 1.4$

Figure 3.- Continued.

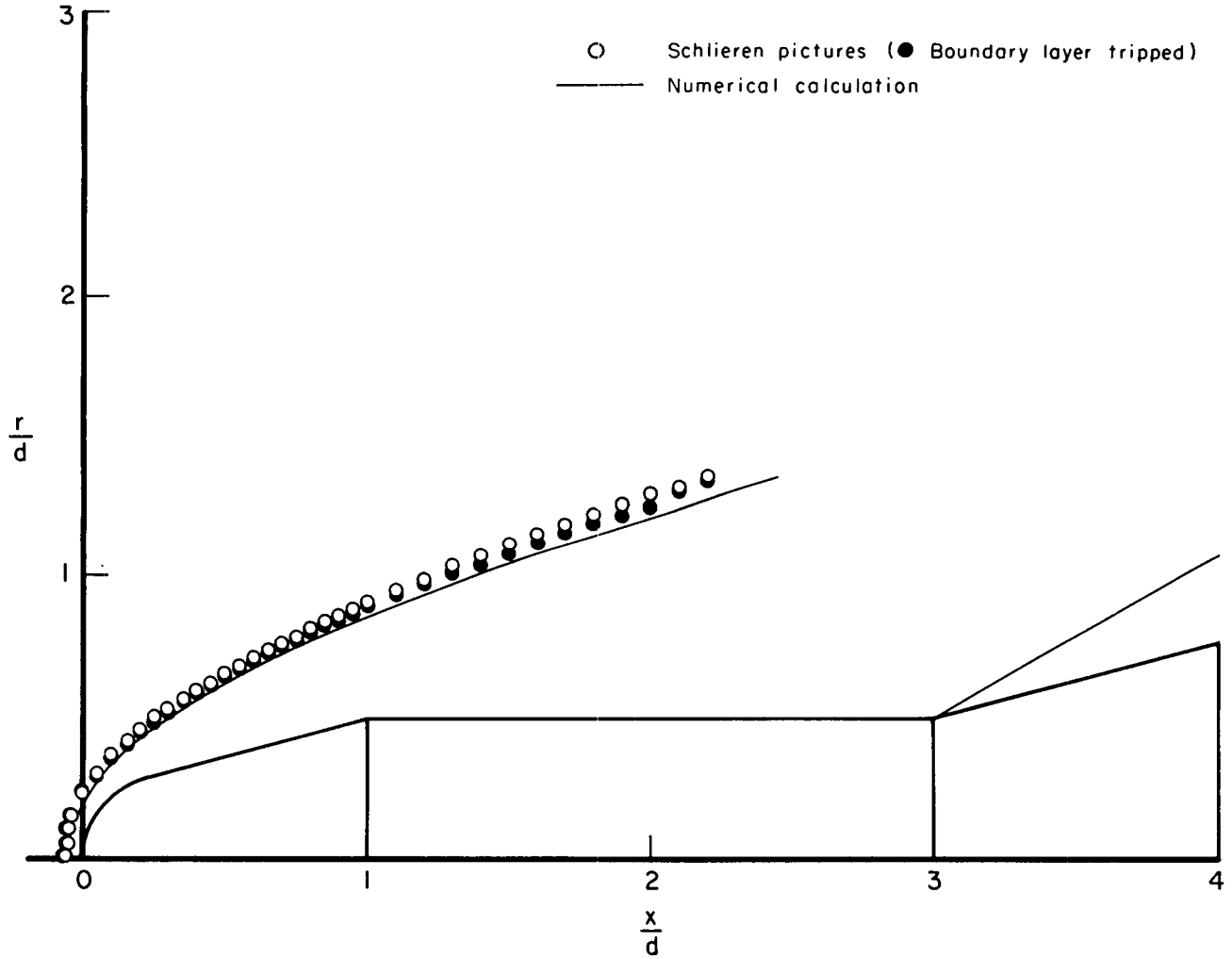

(c) $M_\infty = 5.00$, $\gamma = 1.4$

Figure 3.- Concluded.

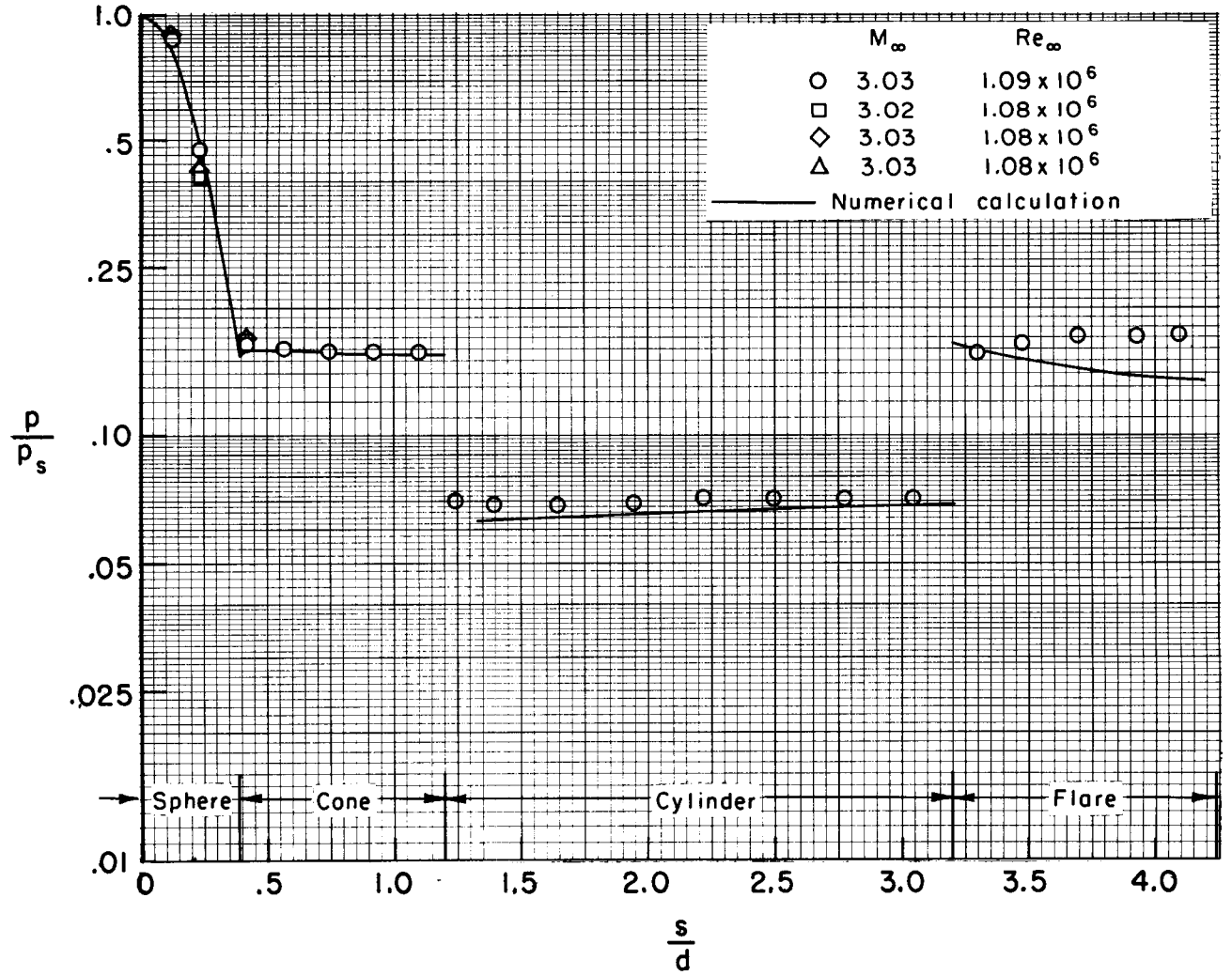

(a) $M_\infty = 3.03$

Figure 4.- Comparison of measured pressures with theoretical predictions.

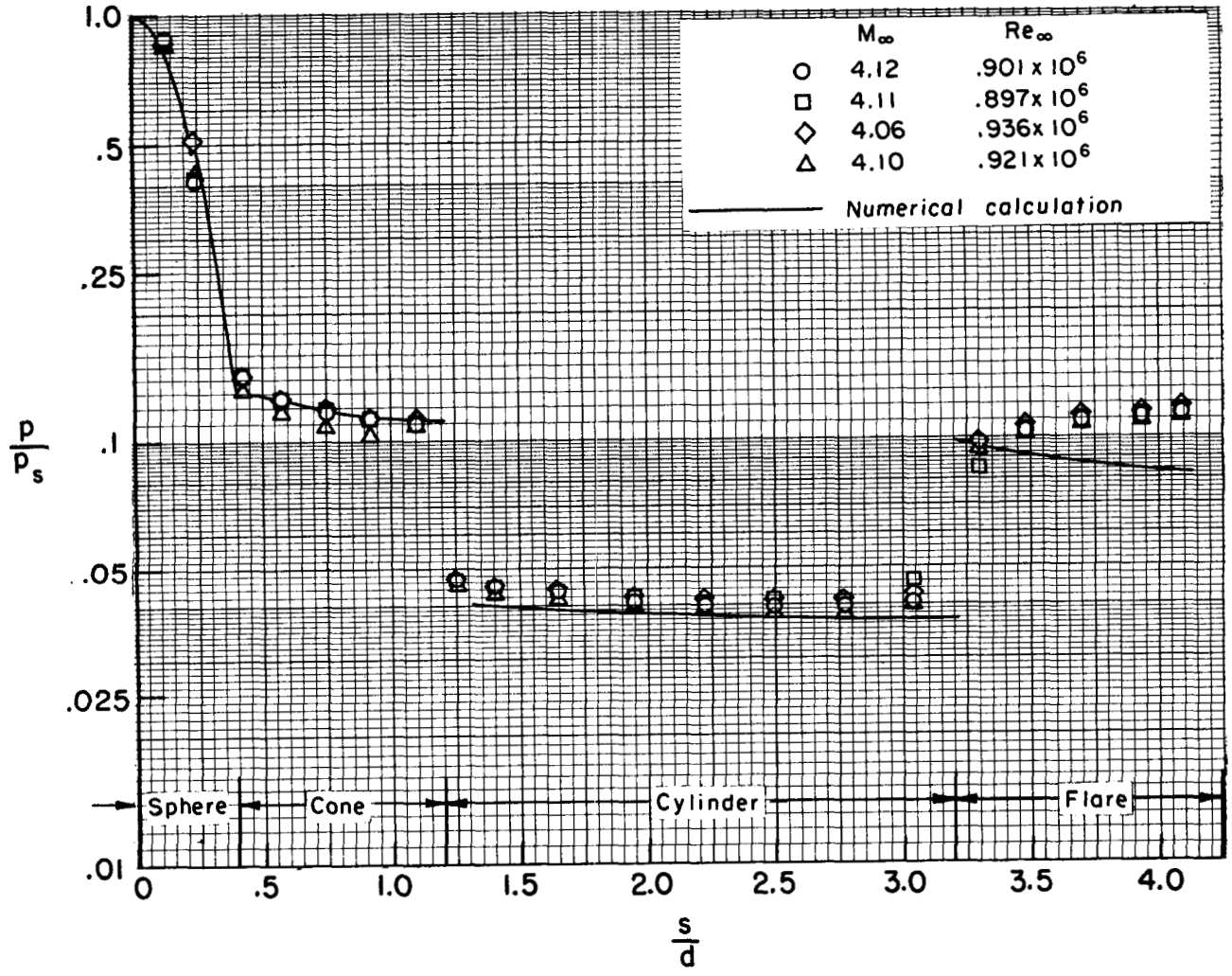

(b) $M_\infty = 4.10$

Figure 4.- Continued.

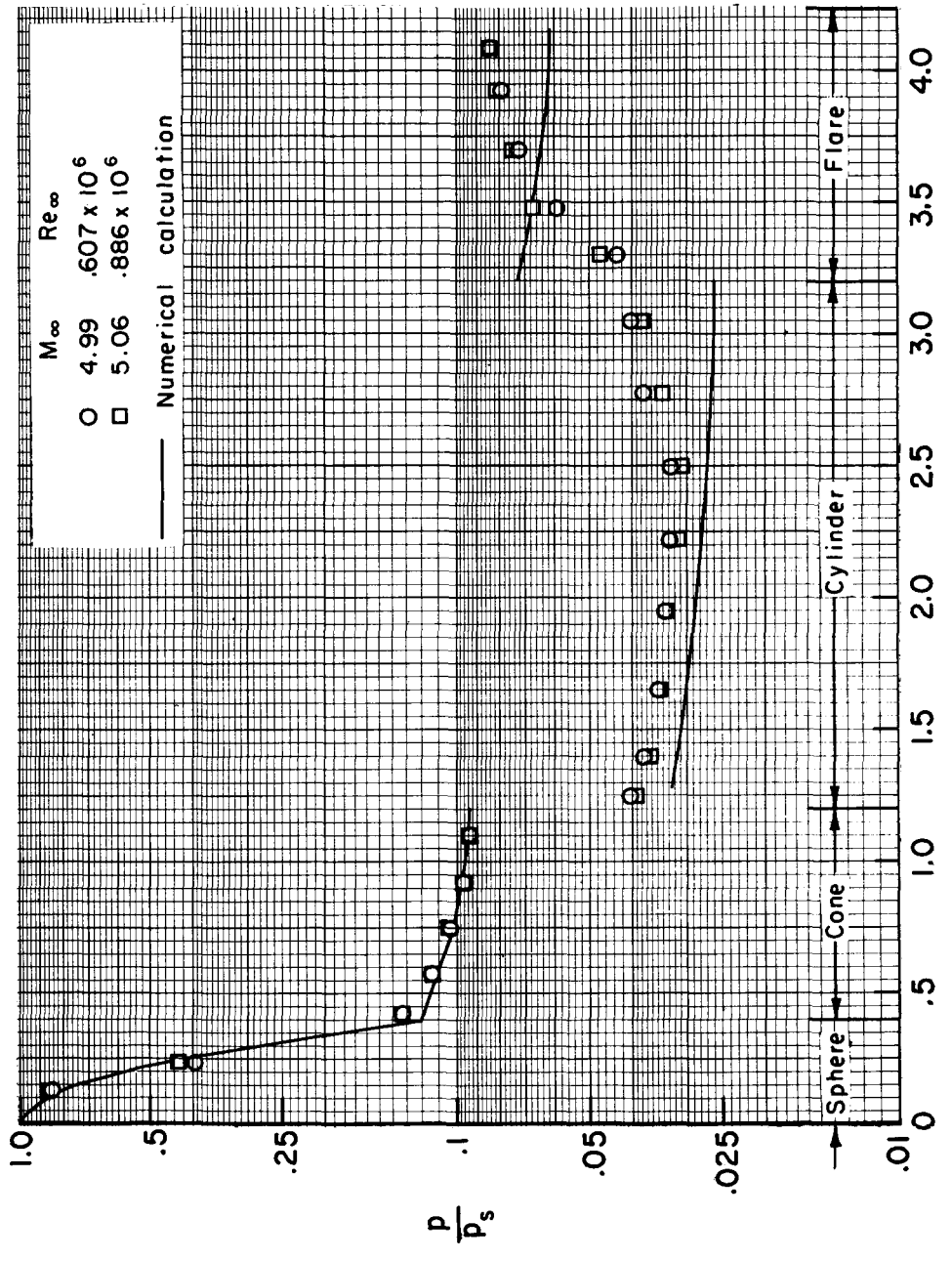

(c) $M_\infty = 5.00$

Figure 4.- Concluded.

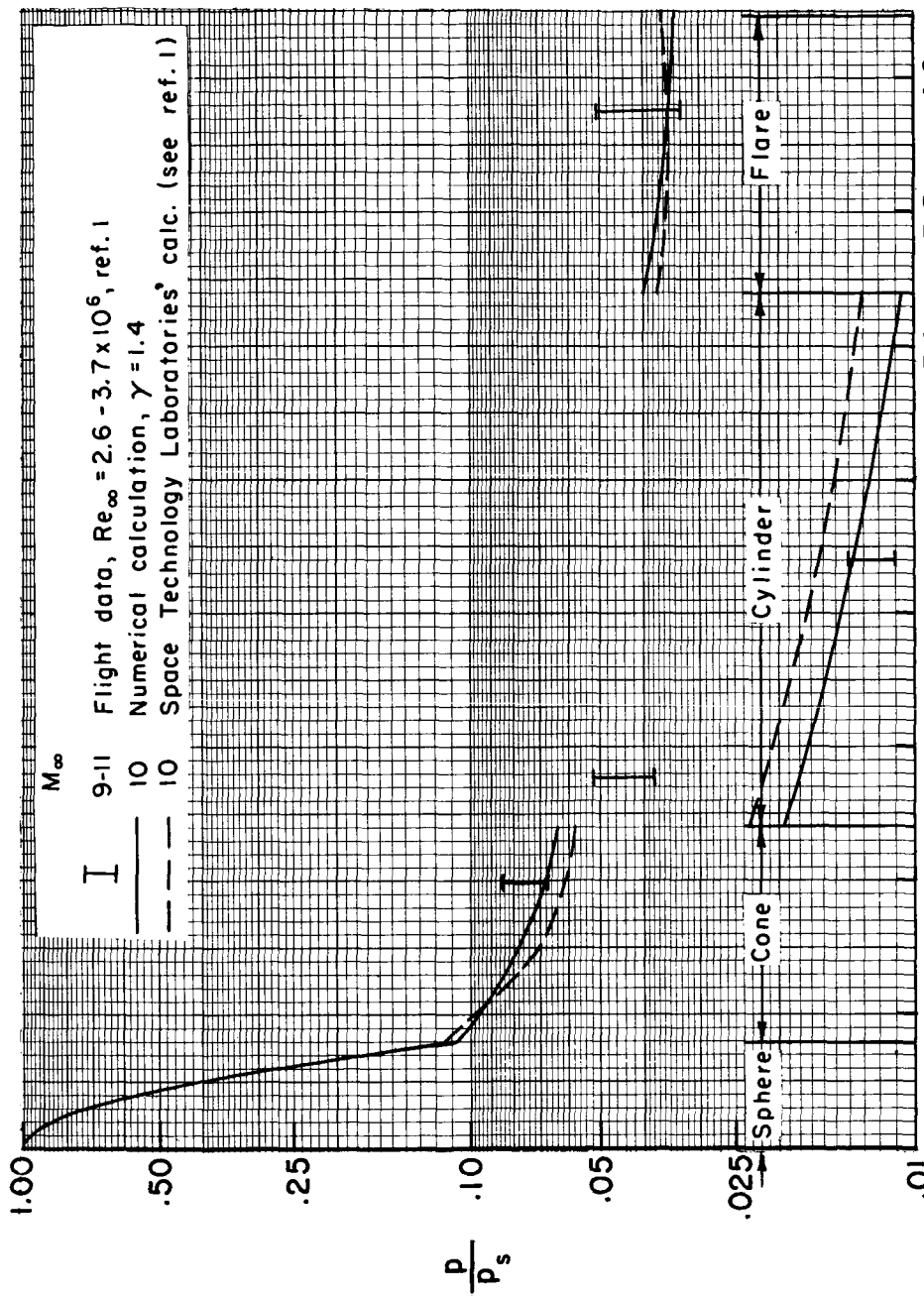

Figure 5.- Comparison of pressures measured on flight model with theoretical predictions.

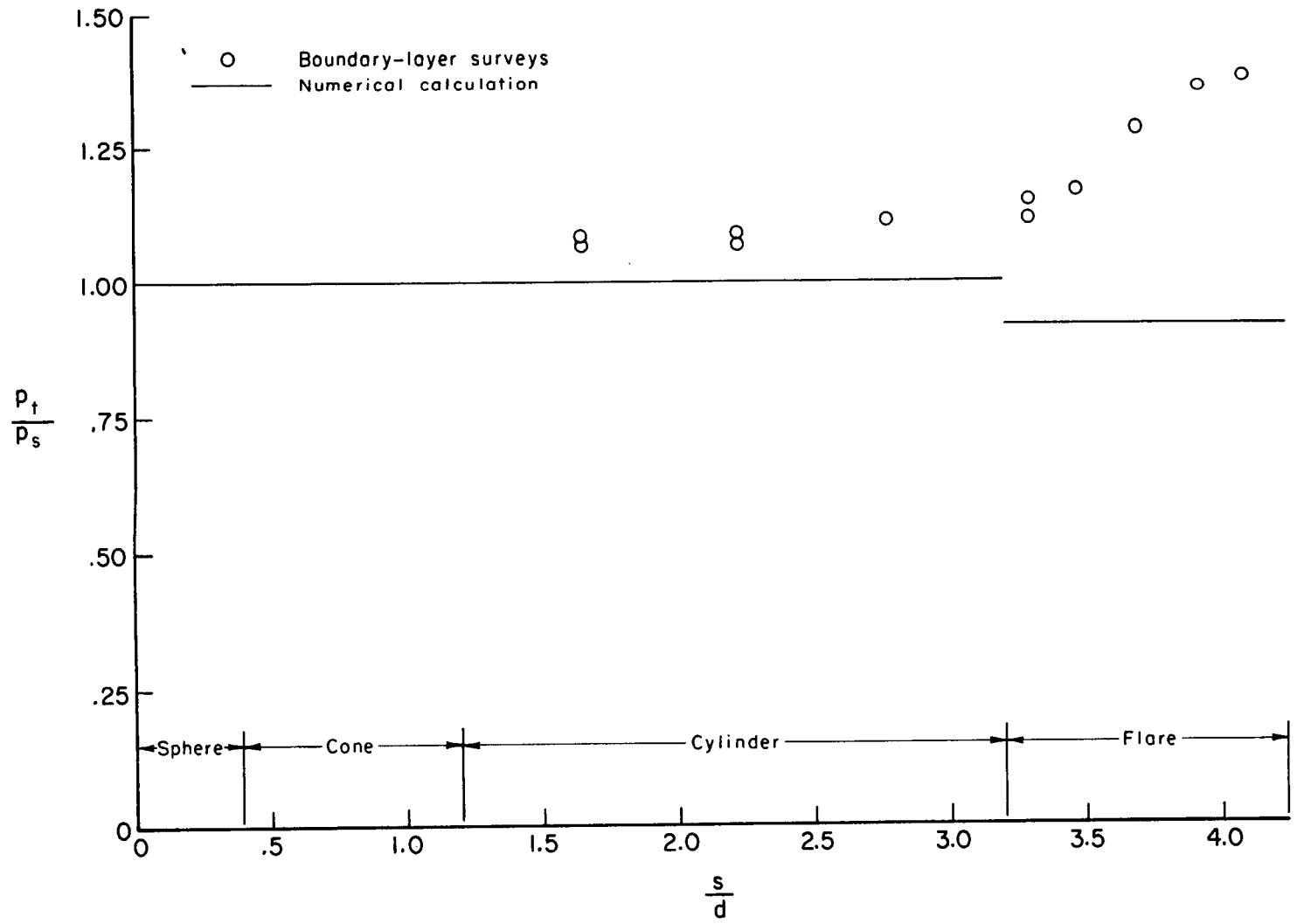

Figure 6.- Comparison of total pressure measured at outer edge of boundary layer with predicted value; $M_\infty = 3.03$, $Re_\infty = 1.08 \times 10^6$.

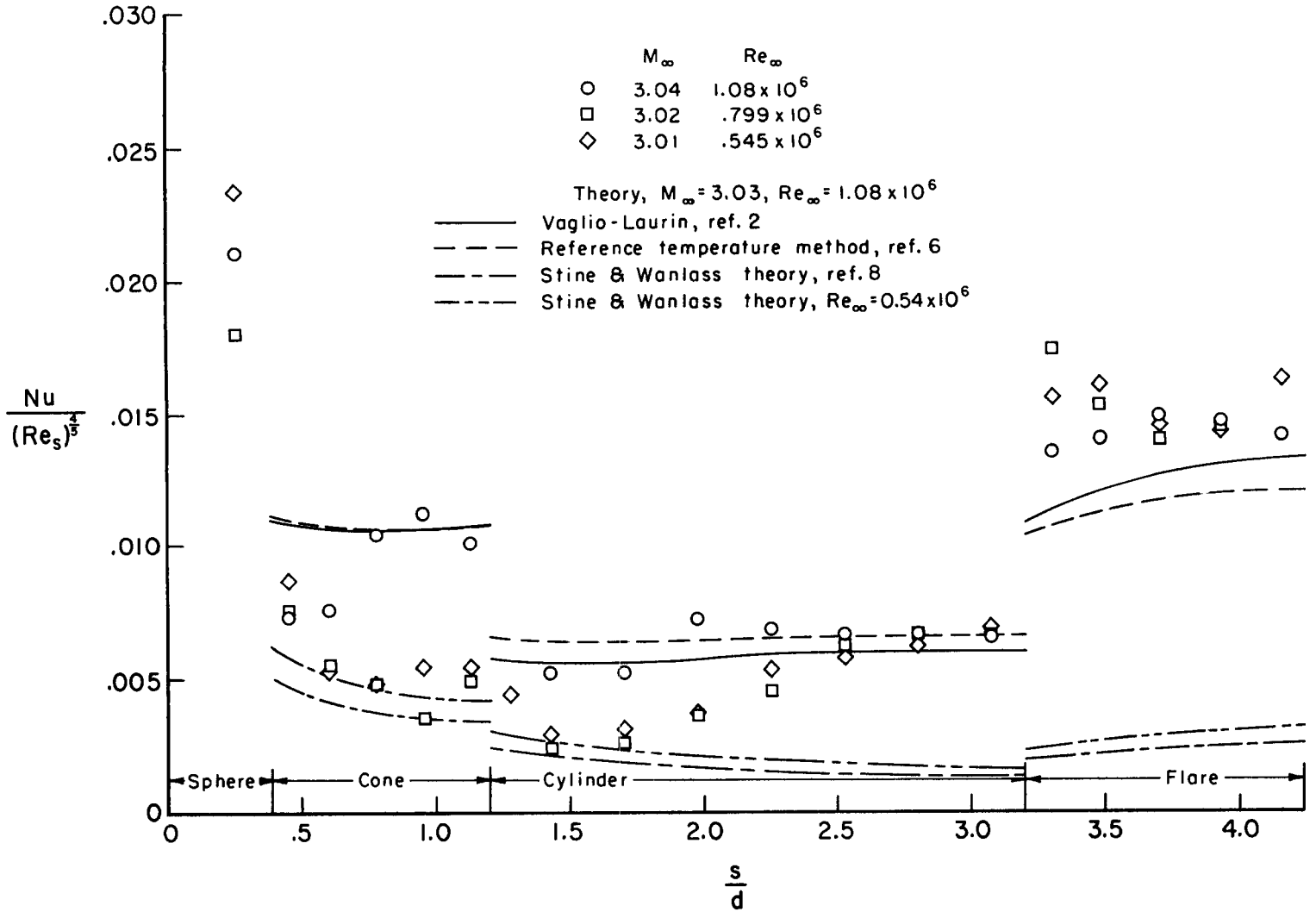

Figure 7.- Comparison of heat-transfer distribution along the model with theoretical predictions.

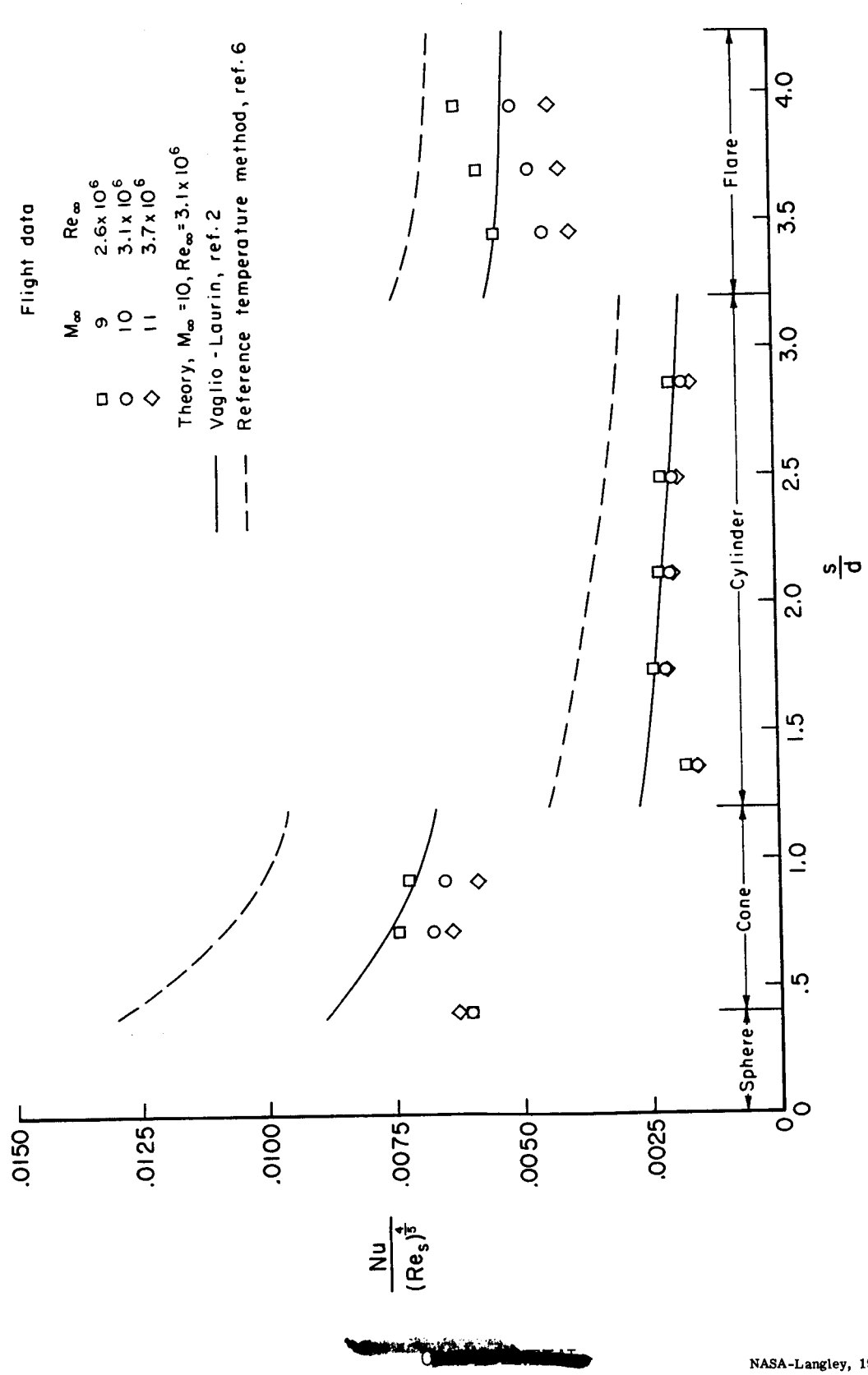

Figure 8.- Comparison of heat-transfer distribution on the flight model with theoretical predictions.